Supporting Information

Photocatalytic Degradation of Aromatic Pollutants: a Pivotal Role of e_{cb}^- in Distribution of Hydroxylated Intermediates

Yue Li, Bo Wen, Wanhong Ma, Chuncheng Chen, and Jincai Zhao*

Beijing National Laboratory for Molecular Sciences, Key Laboratory of Photochemistry, Institute of Chemistry, The Chinese Academy of Sciences, Beijing 100190, China

E-mail: ccchen@iccas.ac.cn

Details of the reduction potential calculation about HO-adduct radicals. The B3LYP/6-31+G(d) method was used for the gas phase geometry optimizations and frequency calculations. The Gibbs free energy of each species was calculated using the B3LYP/6-311++G(2df,2p) electronic energy and the zero-point vibrational energy and thermal corrections (0 → 298 K) obtained at B3LYP/6-31+G(d) level (unscaled). We employed the most recent version of the polarized continuum solvation model (PCM), that is, integral equation formalism PCM (IEF-PCM)[1] to calculate the solvation free energies (with the gas-phase optimized structures and the radii scale factor of 1.2[2-4]). The single-point PCM calculations were also performed at B3LYP/6-311++G(2df,2p) level. The standard reduction potentials (E^0 vs. NHE) of HO-adduct radicals were obtained by

$$E^0 = (G_r - G_a + \Delta G_{rsol} - \Delta G_{asol}) \times 27.2116 - 4.44 \qquad (1),$$

where G_r, G_a, ΔG_{rsol} and ΔG_{asol} are the Gibbs free energies and solvation free energies of the HO-adduct radical and its corresponding anion, respectively. The last term, -4.44 (unit: V) is the free energy change associated with the reference NHE half-reaction ($2H^+(aq) + 2e^-(g) \rightarrow H_2(g)$).[5,6] The results were further corrected by adding 0.28 V, because the B3LYP/6-311++G(2df,2p)//B3LYP/6-31+G(d) method systematically underestimates the adiabatic electron affinity by 0.28 eV.[7]

Estimation about the reduction potential of e_{cb}^-. For colloidal TiO_2, the reduction potential of e_{cb}^- (*i.e.* the quasi-Fermi level of e_{cb}^-) expressed with respect to NHE varies with the pH value of the suspension according to[8]

$$E(e_{cb}^-)^0 = -0.13 - 0.059\text{pH (vs. NHE)} \qquad (2).$$

Table S1. The reported relative yields of *m*-, *p*- and *o*-HO-BAs formed in the photocatalytic oxidation of BA

entry	*m*- (%)	*p*- (%)	*o*- (%)	reference
1	26	25	49	9
2	52	34	14	10
3	44	23	33	11
4	29	28	43	12
5[a]	36	64	---	13

[a] *o*-HO-BA was detected but not quantified in this study, so in the calculations about the relative yields of *p*- and *m*-HO-BAs, the concentration of *o*-HO-BA is not counted in.

Table S2. The relative yields of *m*-, *p*- and *o*-hydroxylated products formed in the photocatalytic oxidation of BA and NB[a]

entry	condition	time	*m*- (%)	*p*- (%)	*o*- (%)
1a	20 mM BA, 0.1 atm O_2	45 min	63.5	16.5	20.0
1b	20 mM BA, 0.1 atm O_2	90 min	63.7	16.9	19.4
2a	20 mM BA, 0.2 atm O_2	45 min	58.5	18.6	22.9
2b	20 mM BA, 0.2 atm O_2	90 min	58.8	19.0	22.2
3a	20 mM BA, 0.4 atm O_2	45 min	53.6	21.5	25.0
3b	20 mM BA, 0.4 atm O_2	90 min	54.3	21.8	23.9
4a	20 mM BA, 0.6 atm O_2	45 min	51.8	23.3	24.9
4b	20 mM BA, 0.6 atm O_2	90 min	51.9	23.5	24.6
5a	20 mM BA, 0.8 atm O_2	45 min	50.1	24.1	25.8
5b	20 mM BA, 0.8 atm O_2	90 min	51.1	24.0	25.0
6a	20 mM BA, 1.0 atm O_2	45 min	49.5	24.6	25.9
6b	20 mM BA, 1.0 atm O_2	90 min	50.5	24.6	24.9

7a	20 mM BA, 2.0 atm O_2	45 min	47.0	25.7	27.3
7b	20 mM BA, 2.0 atm O_2	90 min	47.1	26.5	26.4
8a	5 mM NB, 0.1 atm O_2	45 min	62.9	26.0	11.1
8b	5 mM NB, 0.1 atm O_2	90 min	63.3	25.5	11.2
9a	5 mM NB, 0.2 atm O_2	45 min	46.9	31.1	22.0
9b	5 mM NB, 0.2 atm O_2	90 min	47.3	30.5	22.2
10a	5 mM NB, 1.0 atm O_2	45 min	42.7	33.9	23.4
10b	5 mM NB, 1.0 atm O_2	90 min	43.2	33.8	23.0
11a	1 mM BA, air	45 min	52.5	24.9	22.6
11b	1 mM BA, air	90 min	53.9	24.6	21.5
12a	2 mM BA, air	45 min	53.5	24.3	22.2
12b	2 mM BA, air	90 min	54.1	25.2	20.7
13a	5 mM BA, air	45 min	55.5	22.5	22.0
13b	5 mM BA, air	90 min	55.3	23.3	21.4
14a	10 mM BA, air	45 min	56.7	21.0	22.3
14b	10 mM BA, air	90 min	56.1	22.1	21.8
15a	15 mM BA, air	45 min	57.8	19.6	22.6
15b	15 mM BA, air	90 min	57.5	20.3	22.2
16a	20 mM BA, air	45 min	58.7	19.4	21.9
16b	20 mM BA, air	90 min	57.8	19.2	23.0
17a	saturated BA (~25 mM), air	45 min	59.3	17.8	22.9
17b	saturated BA (~25 mM), air	90 min	58.1	18.2	23.7
18a[b]	20 mM BA, F-TiO_2	45 min	38.9	22.2	38.9
18b[b]	20 mM BA, F-TiO_2	90 min	39.9	21.4	38.7

[a] 1 g/L TiO_2 (P25), 50 mL H_2O. [b] 1 g/L F-TiO_2.

Table S3. The calculated reduction potentials (E^0 vs. NHE) of the HO-adduct radicals of BA and NB in H_2O, and the reduction potentials of the e_{cb}^- of TiO_2 ($E(e_{cb}^-)^0$) at the pH of the photocatalytic systems

HO-adduct radical	E^0 (V)	pH	$E(e_{cb}^-)^0$ (V)
***m*-HO-BA**	-0.66		
***p*-HO-BA**	-0.22	2.7[a]	-0.29
***o*-HO-BA**	-0.27		
***m*-HO-NB**	-0.39		
***p*-HO-NB**	0.34	3.3[b]	-0.32
***o*-HO-NB**	0.31		

[a] 2 g/L TiO_2, 20 mM BA, 5 mL H_2O. [b] 2 g/L TiO_2, 0.5 mL NB, 5 mL H_2O.

Table S4. Percentages of ^{18}O in the hydroxyl groups of HO-BAs formed in $^{16}O_2$(air)/$H_2{}^{18}O$/$H_2{}^{16}O_2$/BA/UV systems[a]

entry	time	*m*- (%)	*p*- (%)	*o*- (%)
1	1 h	2.3	2.6	3.2
2	2 h	2.3	3.1	3.4

[a] 20 mM BA, 10 mM $H_2{}^{16}O_2$, 1 mL $H_2{}^{18}O$, irradiation time: 1 and 2 h.

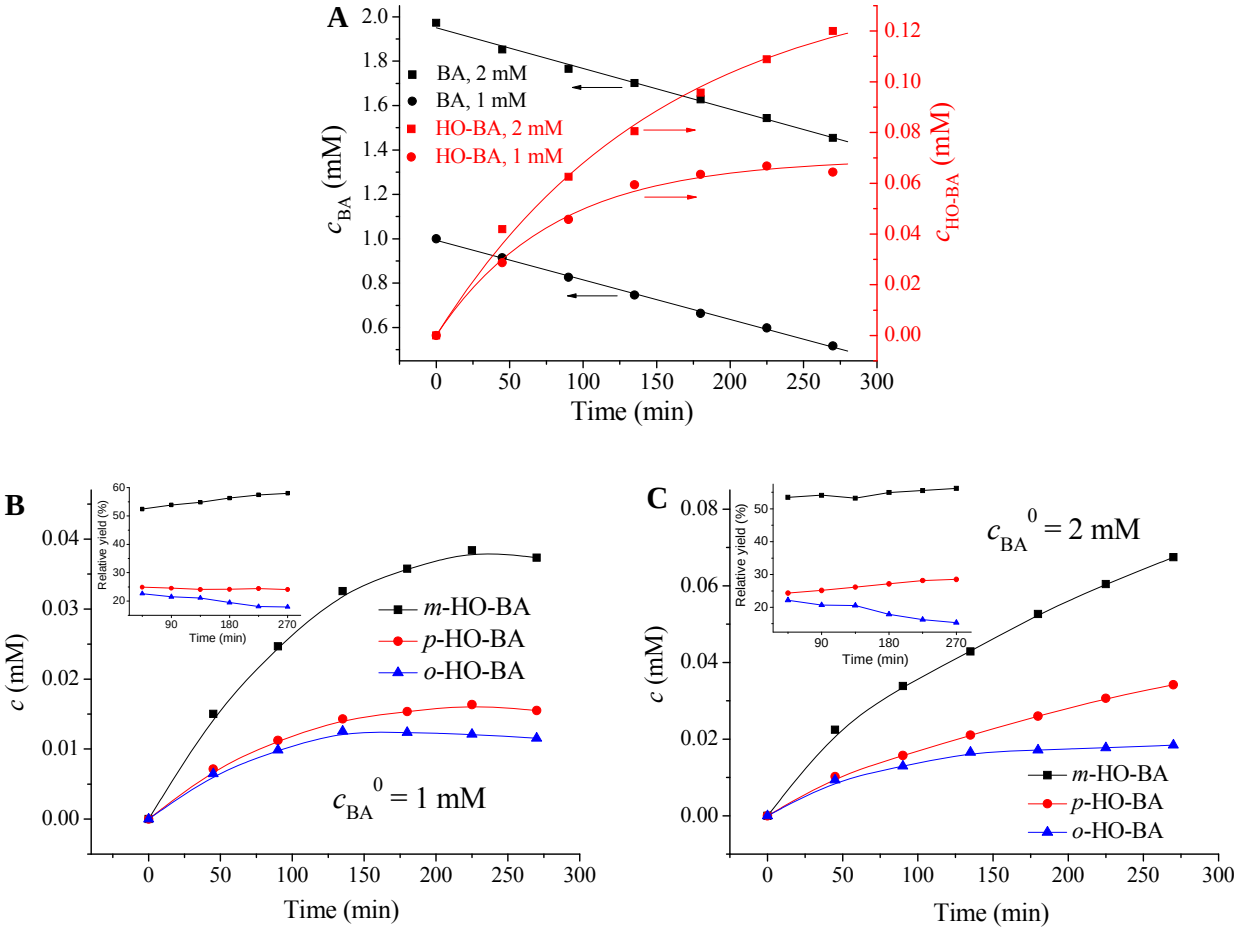

Figure S1. (A) Consumption of BA (black) and total yield of monohydroxylated products (red) during the photocatalytic degradation of BA with initial concentration of 1 (circle) and 2 mM (square). (B) and (C) The concentrations of *m*-, *p*- and *o*-HO-BAs in the 1 and 2 mM BA systems, respectively. Insets of (B) and (C): the corresponding relative yields of HO-BAs.

As shown by the black straight lines in Figure S1A, the degradation of BA follows zero-order kinetics. The apparent consumption rate constants of BA were 1.78 and 1.83 μM/min for the systems with initial BA concentration of 1 and 2 mM, respectively, indicating that the consumption rate of the substrate is not remarkably affected by its initial concentration. However, the accumulation of HO-BAs was observed to be largely facilitated by the increase of initial substrate concentration. For example, at irradiation of 90 min, the total concentration of three HO-BAs was 45.8 μM with initial BA concentration of 1 mM and 62.5 μM in the case of 2 mM. The accumulation of HO-BAs is determined

by their formation and consumption during the reaction. The formation and consumption of HO-BAs were tentatively fitted with zero-order and first-order reactions, respectively. As shown by the red lines, such a fitting was in well agreement with experimental data. The apparent formation rate constants of HO-BAs were 0.874 and 0.925 μM/min for the 1 and 2 mM BA systems, respectively, which is consistent with the similarity in the consumption rate of BA. In both systems, the total formation rate of HO-BAs accounts for ca. 50% of the consumption rate of BA, which means that they are the main primary photocatalytic oxidation products of BA. In contrast to the formation, the consumption rate constant of HO-BAs for the 2 mM BA system (0.0065 min^{-1}) was much lower than that with 1 mM BA (0.0126 min^{-1}), indicating that the effect of initial BA concentration on the accumulation of HO-BAs is mainly due to its influence on the consumption, rather than the formation of them. It is obvious that high initial substrate concentration inhibits the secondary reactions of hydroxylated intermediates, which is probably caused by the competition between BA and HO-BAs for surface adsorption sites and reactive species.

Figures S1B and S1C illustrate the individual concentrations of three HO-BAs in the 1 and 2 mM BA systems, respectively. It is obvious that the accumulation of each HO-BA slowed down with reaction time in both systems, indicating that their secondary reactions become more significant when reaction time is prolonged. The insets of Figures S1B and S1C illustrate the relative yields of HO-BAs (the ratios of the individual concentration of one HO-BA to the total concentration of three HO-BAs). Although the relative yields of HO-BAs changed slowly with reaction time, their relative yields of 45 and 90 min reactions were generally very close. For example, in the 2 mM BA system, the relative yield differences of *m*-, *p*- and *o*-HO-BAs between 45 and 90 min reactions were 0.6%, 0.8% and 1.4%, respectively. It is indicated that, during the first 90 min of the reaction, the yield distribution of HO-BAs is stable and not remarkably affected by their secondary reactions. Due to the inhibition of BA on the secondary reactions of its hydroxylated products, it is expected that the effect of secondary reactions on the yield distribution of HO-BAs would become more insignificant at higher substrate concentrations (5-25 mM in this study).

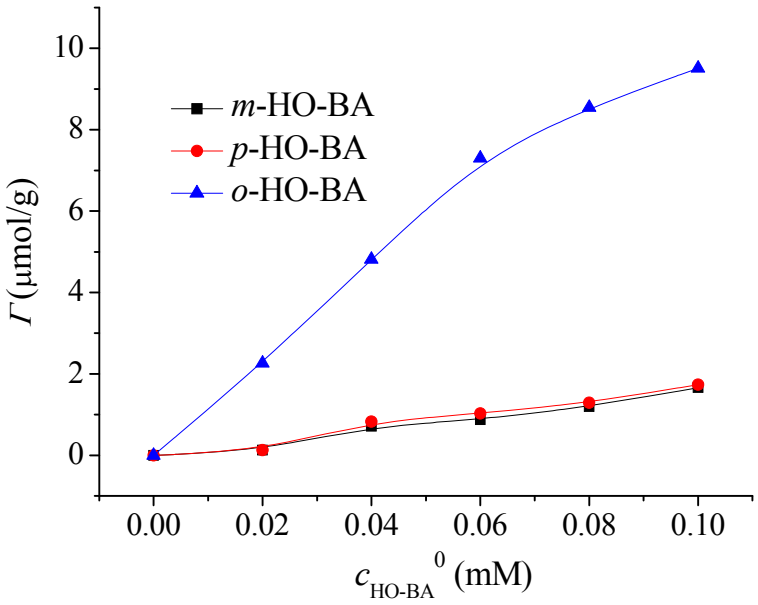

Figure S2. Adsorption amounts of *m*-, *p*- and *o*-HO-BAs in the presence of BA. 5 g/L TiO_2 (P25), c_{BA}^{0} = 10 mM.

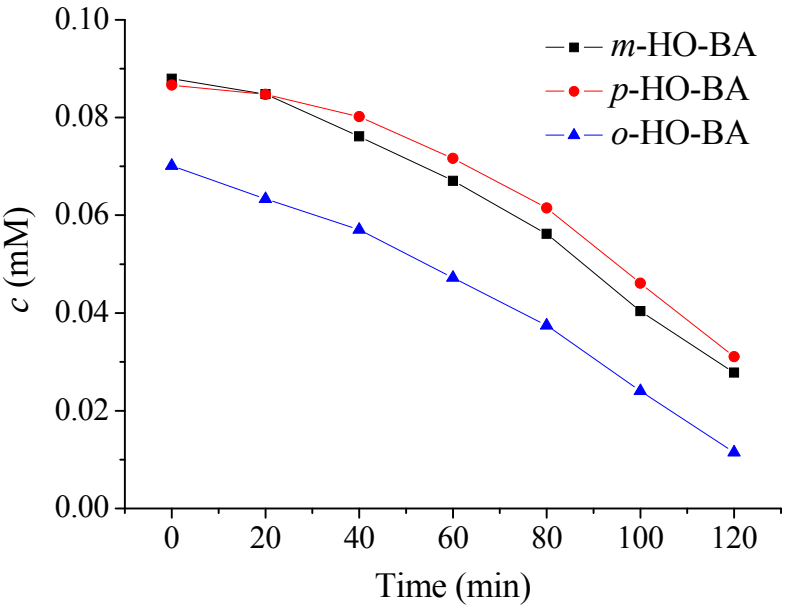

Figure S3. Photocatalytic degradation of *m*-, *p*- and *o*-HO-BAs.1 g/L TiO_2 (P25), $c_{m\text{-HO-BA}}^{0}$ = 0.1 mM, $c_{p\text{-HO-BA}}^{0}$ = 0.1 mM, $c_{o\text{-HO-BA}}^{0}$ = 0.1 mM.

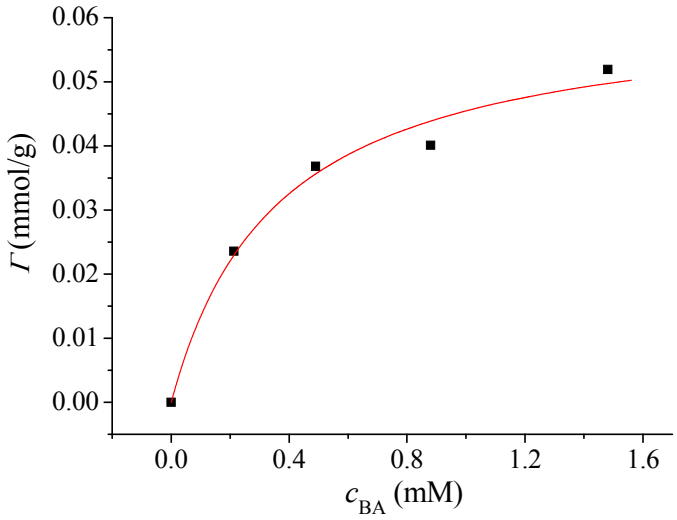

Figure S4. Adsorption isotherm of BA on TiO_2. 10 g/L TiO_2 was dispersed in the solutions of BA with concentration from 0.2 to 1.5 mM. The suspensions were stirred for 8 h in the dark to achieve adsorption-desorption equilibrium. The concentrations of BA, before and after adsorption were determined by HPLC method, and quantified from its absorbance at 230 nm. The relationship between the concentration of BA and the adsorbed amount was correlated with the Langmuir isotherm. The obtained maximum adsorbed amount (Γ_{max}) was 0.062 mmol/g, and the adsorption constant (K) was 2.78 mM^{-1}. This result is in well agreement with the reported values.[14]

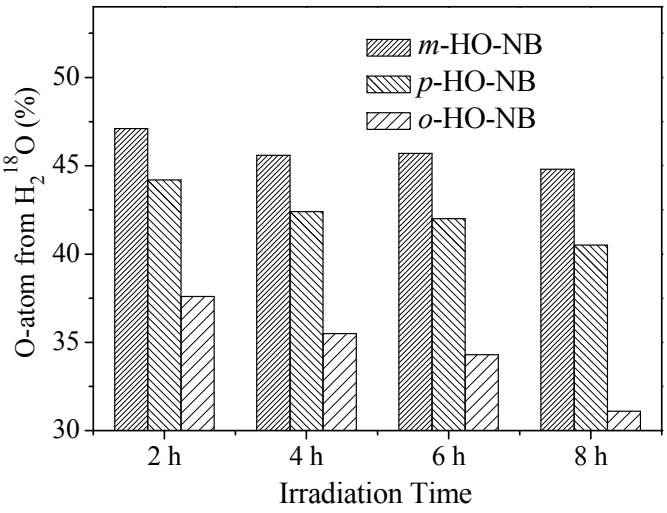

Figure S5. Abundances of ^{18}O in the hydroxyl groups of HO-NBs formed in the photocatalytic oxidation of NB, using aerial $^{16}O_2$ as oxidant and $H_2{}^{18}O$ as solvent. 2 g/L TiO_2 (P25), 1 mL $H_2{}^{18}O$, 100 μL NB.

REFERENCES

(1) Cossi, M.; Scalmani, G.; Rega, N.; Barone, V. New developments in the polarizable continuum model for quantum mechanical and classical calculations on molecules in solution. *J. Chem. Phys.* **2002,** *117*, 43-54.

(2) Barone, V.; Cossi, M.; Tomasi, J. A new definition of cavities for the computation of solvation free energies by the polarizable continuum model. *J. Chem. Phys.* **1997,** *107*, 3210-3221.

(3) Cammi, R.; Mennucci, B.; Tomasi, J. On the calculation of local field factors for microscopic static hyperpolarizabilities of molecules in solution with the aid of quantum-mechanical methods. *J. Phys. Chem. A* **1998,** *102*, 870-875.

(4) Cammi, R.; Mennucci, B.; Tomasi, J. An attempt to bridge the gap between computation and experiment for nonlinear optical properties: Macroscopic susceptibilities in solution. *J. Phys. Chem. A* **2000,** *104*, 4690-4698.

(5) Evans, D. H. One-electron and two-electron transfers in electrochemistry and homogeneous solution reactions. *Chem. Rev.* **2008,** *108*, 2113-2144.

(6) Trasatti, S. The absolute electrode potential: An explanatory note. *Pure Appl. Chem.* **1986,** *58*, 955-966.

(7) Fu, Y.; Liu, L.; Yu, H.-Z.; Wang, Y.-M.; Guo, Q.-X. Quantum-chemical predictions of absolute standard redox potentials of diverse organic molecules and free radicals in acetonitrile. *J. Am. Chem. Soc.* **2005,** *127*, 7227-7234.

(8) Dung, D.; Ramsden, J.; Graetzel, M. Dynamics of interfacial electron-transfer processes in colloidal semiconductor systems. *J. Am. Chem. Soc.* **1982,** *104*, 2977-2985.

(9) Matthews, R. W. Hydroxylation reactions induced by near-ultraviolet photolysis of aqueous titanium-dioxide suspensions. *J. Chem. Soc., Faraday Trans. I* **1984,** *80*, 457-471.

(10) Brezova, V.; Ceppan, M.; Brandsteterova, E.; Breza, M.; Lapcik, L. Photocatalytic hydroxylation of benzoic-acid in aqueous titanium-dioxide suspension. *J. Photochem. Photobiol., A* **1991,** *59*, 385-391.

(11) Chan, A. H. C.; Chan, C. K.; Barford, J. P.; Porter, J. F. Solar photocatalytic thin film cascade reactor for treatment of benzoic acid containing wastewater. *Water Res.* **2003,** *37*, 1125-1135.

(12) Palmisano, G.; Addamo, M.; Augugliaro, V.; Caronna, T.; Di Paola, A.; Lopez, E. G.; Loddo, V.; Marci, G.; Palmisano, L.; Schiavello, M. Selectivity of hydroxyl radical in the partial oxidation of aromatic compounds in heterogeneous photocatalysis. *Catal. Today* **2007,** *122*, 118-127.

(13) Velegraki, T.; Mantzavinos, D. Conversion of benzoic acid during TiO_2-mediated photocatalytic degradation in water. *Chem. Eng. J.* **2008,** *140*, 15-21.

(14) Moser, J.; Punchihewa, S.; Infelta, P. P.; Gratzel, M. Surface complexation of colloidal semiconductors strongly enhances interfacial electron-transfer rates. *Langmuir* **1991,** *7*, 3012-3018.